ELSEVIER

9 May 1997

Chemical Physics Letters 269 (1997) 479–484

CHEMICAL PHYSICS LETTERS

Growth manipulation in electrodeposition with self-assembled monolayers

Ornella Cavalleri, Scott E. Gilbert, Klaus Kern

Institut de Physique Expérimentale, Ecole Polytechnique Fédérale de Lausanne, CH-1015 Lausanne, Switzerland

Received 29 November 1996; in final form 13 March 1997

Abstract

A novel approach for manipulating the morphology and growth mode of metal electrodeposits based on the controlled modification of the electrode surface by self-assembled monolayers is introduced. Au(111) electrodes have been modified with alkanethiols of varying chain length and the electrodepositon of copper overlayers has been monitored by in situ electrochemical scanning tunneling microscopy. Through systematic control of the electrode potential and thiol chain length we can deposit two-dimensional copper clusters, three-dimensional copper nodules or grow smooth copper layers.

There is increasing interest in developing methods for the precise control of the growth morphology of thin epitaxial films on the microscopic scale [1,2]. The basic goal of epitaxial film growth, in vacuum as well as in solution, is the growth of flat defect-free films of specified crystallographic surface orientation. Several approaches have been developed, mainly based on the control of growth kinetics, to grow such films with smooth abrupt interfaces. A particularly appealing approach for manipulating the growth kinetics and to force a smooth layer-by-layer growth is the deliberate introduction of impurities, so called surfactants or additives. While their use in molecular beam epitaxy has only recently been explored [3], it has long been common knowledge in the metal plating industry that certain organic compounds, known there as leveling agents, in the plating bath will favor smooth electrodeposition [4,5].

In this Letter we introduce an alternative approach for the microscopic control of the electrocrystallization of metals which is based on the chemical modification of the electrode surface. Copper overlayers have been deposited on Au(111) electrodes which were modified with self-assembled alkanethiol monolayers of varying chain length and the growth mechanism has been monitored by in situ electrochemical scanning tunneling microscopy (STM). Self-assembled monolayers (SAM) have been advantageously used in electrochemistry to obtain well ordered and defined electrochemical interfaces which have found applications in basic and applied research fields, from charge transfer to corrosion inhibition [6]. Although the possibility of using these organic films to manipulate and control the electrocrystallization of metals on the electrode surface suggests itself, this aspect is unexplored.

Our in situ STM study reveals that through systematic control of the electrode potential and SAM thickness we can manipulate the growth morphology and deposit two-dimensional copper clusters, three-dimensional copper nodules or grow copper layers in a quasi two-dimensional growth mode. Indepen-

PII S0009-2614(97)00317-5

dently of the chain length, in the underpotential deposition (UPD) region [1] we observe the formation of two-dimensional Cu islands 2–5 nm in diameter. The clusters are homogeneously distributed at the surface and their density reaches its maximum in the UPD region. In the overpotential deposition (OPD) region a chain length dependent behavior is observed. For alkanethiol chain lengths up to 12 carbon atoms, two-dimensional growth is obtained in the potential region where bulk three-dimensional deposition is expected to occur on the clean electrode. Layered growth occurs by diffusion limited growth and subsequent coalescence of the copper cluster nuclei originally formed in the UPD region. The further formation of a second and third copper layer has been observed to occur in the same manner as the first (quasi two-dimensional type growth). For longer chain lengths ($n > 12$), no further growth in the UPD clusters is observed, thus no Cu overlayer develops.

Alkanethiol monolayers were formed by self-assembly in a 1 mM solution. The Au(111) samples were epitaxially grown on mica in a high-vacuum, flame annealed in a hydrogen flame, quenched in ethanol and while still covered by ethanol transferred into the thiol solution, where they were kept at least 15 h [7]. After preparation of the SAM the sample has been rinsed with ethanol, dried in an argon flow and dipped into the electrolyte before being transferred to the STM. The microscope is a homebuilt variable temperature beetle-type STM which was equipped with an electrochemical cell to allow in-situ electrochemical STM studies [8]. Particular care has been taken in the preparation of the SAMs in order to obtain well ordered, defect-free monolayers which uniformly cover the whole surface. An important processing step in this regard is the careful annealing of the monolayer after self-assembly at temperatures between 350 and 380 K, or annealing during self assembly at 320 K for 48 h. During the annealing the

Fig. 1. Morphology of a Au(111) surface covered by a decanethiol self-assembled monolayer. After self-assembly the surface has been annealed for three hours at 360 K. The image size is 3000 Å × 3000 Å.

average size of the molecularly ordered domains increases substantially [7]. An example is given in Fig. 1, showing the morphology of a decanethiol monolayer after annealing at 360 K for three hours. Large molecularly ordered domains (~ 400–600 Å in size) separated by domain boundaries, imaged as depression lines, characterize the SAM surface. Some small holes are still present on the terraces. As already reported [9–11], these holes are vacancy islands in the topmost gold layer formed during the initial thiol chemisorption. It is important to note that the holes are covered by molecules as are the surrounding terraces [10]; i.e. they are not pinholes in the SAM. It is due to the careful annealing that the vacancy island density has been largely reduced and a flat surface is obtained [11–13]. The electrochemical measurements were done in 0.05 M H_2SO_4/1 mM $CuSO_4$ electrolyte with potentials referred to the Cu/Cu^{2+} quasi-reference electrode. Shown in Fig. 2a–c are typical cyclovoltammograms taken on bare, hexane- and octadecanethiol-modified Au(111) electrodes.

The electrochemical deposition of Cu on thiol-covered Au(111) electrodes has been chosen because of the considerable amount of data available for the Cu/Au(111) system [14–17] which serves as a database for investigating the role of the SAM in the deposition process. It is well known that the elec-

[1] Underpotential and overpotential deposition regions refer to potentials positive and negative of the thermodynamical potential for Cu/Cu^{2+}. For thiol-covered electrodes, the actual interfacial potential is not known and we use this terminology to refer to regions of the electrode potential where one normally sees UPD and OPD on clean gold.

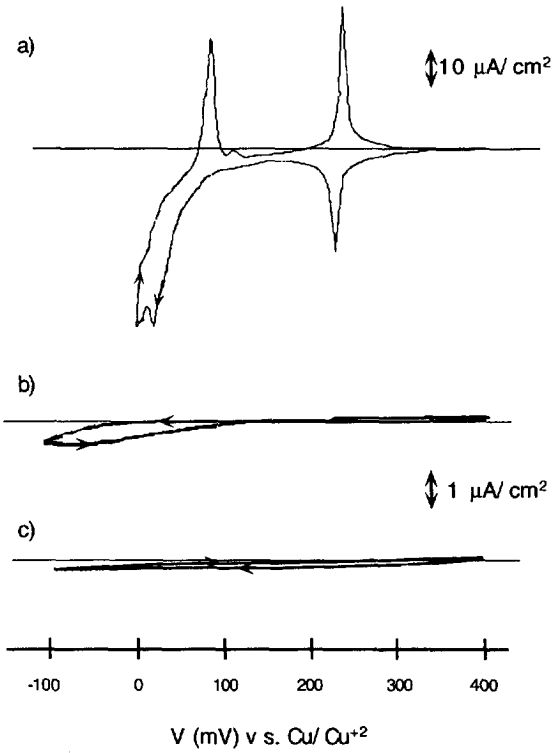

Fig. 2. Cyclovoltammograms of Cu electrodeposition taken in situ in the STM cell on (a) a bare Au(111) electrode; (b) Au(111) covered with a hexanethiol SAM; (c) a Au(111) electrode covered with an octadecanethiol SAM. Scan rate: 5 mV/s. Electrolyte: 0.05 M H_2SO_4 + 1 mM $CuSO_4$, undeaerated. Potential referenced to Cu wire in the same electrolyte (Cu/Cu^{2+}).

trodeposition of Cu on Au(111) proceeds via the formation of a first Cu monolayer in the UPD region, i.e. at potentials positive with respect to the Nernst potential, followed by a 3D bulk deposition of Cu in the OPD region, i.e. at potentials lower than the Nernst potential. The presence of the thiol monolayer substantially modifies the electrodeposition in both regions in UPD [8] as well as in OPD. To illustrate this fact, Cu growth on an octadecanethiol-modified Au surface is shown in Fig. 3. The image sequence shows the evolution of UPD nanocluster growth at a potential of +50 mV. In these images, a front is seen that slowly sweeps across the surface from left to right and top to bottom, at which the clusters nucleate. The clusters are monolayer high Cu islands 2–5 nm in diameter. Once formed, the islands remain fixed on the surface behind the front. The clusters are homogeneously distributed at the surface, i.e. nucleation initiates on top of the terraces, not at step edges nor at other obvious defect sites as is usually the case in electrodeposition. This scenario is common to all the alkanethiols studied, independent of chain length. The cluster density is independent of alkanethiol chain length, and is generally found to be $\sim 1.5 \times 10^{-4}/\text{Å}^2$.

It is interesting to note that UPD Cu islands have been observed on thiol-covered gold electrodes by Sun and Crooks [18]. However, in their pretreatment of the surfaces, the authors subjected the thiol layers to large positive potential excursions to clean the supposed bare areas of the gold surface. It is known that such potential excursions can oxidatively desorb alkanethiols [19,20]. In our study, care has been taken to leave the thiol layers intact avoiding any large excursion of the electrode potential.

In the overpotential range, the nanocluster morphology is stable on the octadecanethiol covered

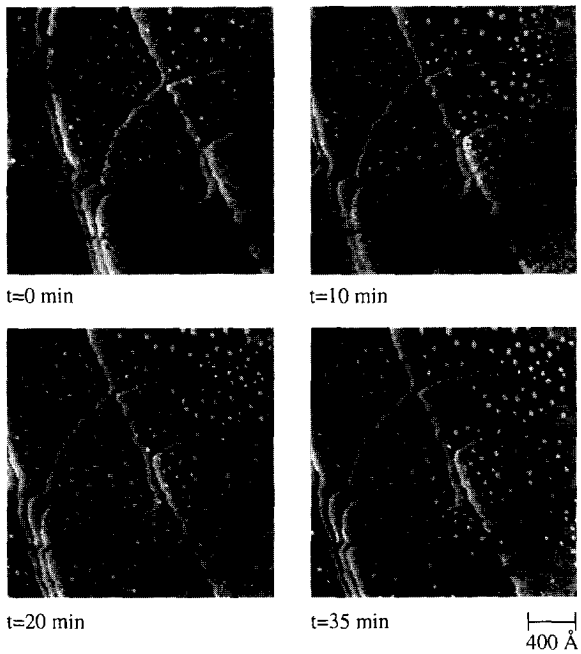

Fig. 3. In situ STM image sequence of the formation of islands in the underpotential range on an octadecanethiol-covered Au(111) electrode. Islands nucleate at the front spreading across the image from left to right. Electrode potential: +50 mV vs. Cu/Cu^{2+} (in the UPD range). Each image is 2150 Å × 2150 Å. Tip bias 120 mV, 0.2 nA tunneling current.

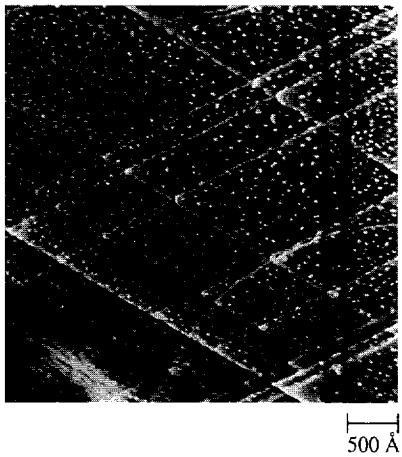

Fig. 4. In situ STM image depicting no further change in the fully developed UPD cluster coverage on an octadecanethiol-covered Au(111) electrode even after several hours at −150 mV vs. Cu/Cu^{2+}. Image size: 3900 Å×3900 Å. Tip bias 200 mV, 0.2 nA tunneling current.

surface, and further deposition of Cu is not observed even at a potential of −150 mV held for several hours (Fig. 4). To see if this lack of growth was due to Cu^{2+} diffusion inhibition caused by the close proximity of the STM tip to the surface, as has been reported in STM studies of Cu electrodeposition [21], we have confirmed that indeed no overpotential deposition occurs anywhere on the electrode surface by a random sampling of various locations on the same sample separated by macroscopic distances.

The inhibitory effect observed in the OPD regime is chain length dependent. While for long chain monolayers ($n > 12$) no further growth occurs at potentials as negative as −200 mV after the initial stage of UPD cluster formation, electrode surfaces covered by short chain monolayers ($n \leqslant 12$) exhibit a two-dimensional layer growth in the OPD region. As an example, we show in Fig. 5 the time evolution of two-dimensional overpotential Cu growth on a hexanethiol layer while keeping the surface potential at −110 mV. Cluster nucleation in the UPD region is the initial phase of Cu layer growth. At overpotentials essentially no further nuclei are formed but the existing Cu clusters grow laterally. At this stage the island density is high enough that each Cu atom has sufficient mobility to reach existing islands with a higher probability than to meet a second mobile atom and to form a new nucleus [22]. As can be seen from the STM images island growth leads to ramification of the islands. In analogy to vapor phase epitaxial growth the "fractal" island shape can be ascribed to the low perimeter mobility for attaching atoms [23,24]. Upon further increase of the coverage, island coalescence sets in finally completing the first monolayer. The formation of the second monolayer starts only when the first one is almost completed. The last image of the sequence in Fig. 5 shows the

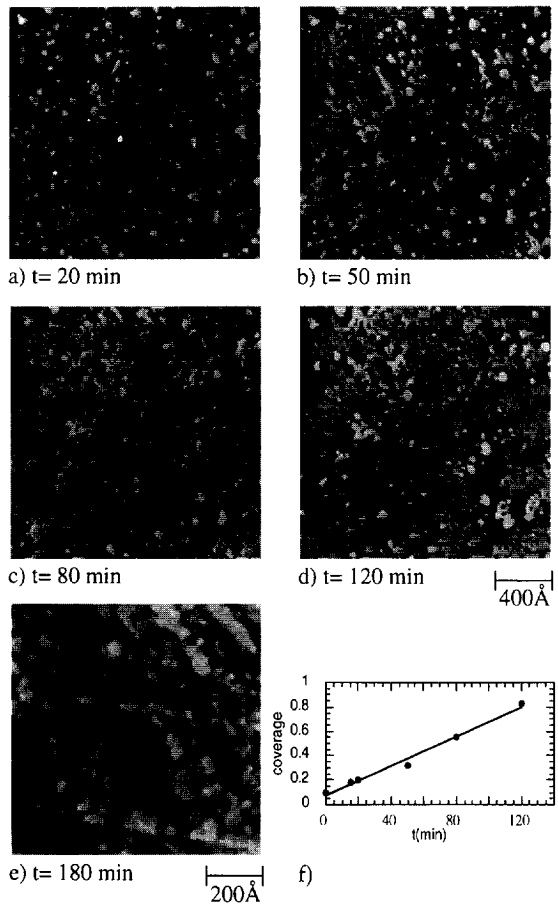

Fig. 5. (a)–(e) In situ electrochemical STM image sequence of Cu electrocrystallization on a hexanethiol-modified Au(111) electrode. Electrolyte: 0.05M H_2SO_4 + 1 mM $CuSO_4$. Electrode potential: −110 mV vs. Cu/Cu^{2+} reference. Tip bias 120 mV, 0.5 nA tunneling current. Image size: (a)–(d) 1750 Å×1750 Å, (e) 880 Å×880 Å. Note that while images (a)–(d) show the same region of the electrode, image (e) is taken at a different spot of the sample. (f) Plot of Cu coverage vs. time.

formation of the second monolayer, which again grows two-dimensionally. Note, however, that some third monolayer islands have nucleated on top. The inset in Fig. 5 shows a plot of the coverage vs. time. This plot is linear, demonstrating that the electrodeposition flux was constant, and equivalent to a deposition current of 45 nA/cm^2 [2].

It is quite remarkable that the evolution of the Cu monolayer on the hexanethiol covered Au surface much resembles the growth scenario of vapor phase epitaxy in the kinetic growth regime. Homogeneous nucleation followed by diffusion limited aggregation and coalescence is the well documented scenario for metal-on-metal growth at low temperatures [22–25]. This electrocrystallization mechanism strongly contrasts the usual behavior of Cu electrodeposition on bare Au(111) with the heterogeneous nucleation of large 3D clusters [5]. For the alkanethiol covered gold surfaces bulk copper nodules could only be deposited at potentials even lower than −200 mV. At these negative surface potentials the sudden growth of big 3D Cu nodules is observed probably due to a breakdown of the thiol layer [8].

The presence of UPD islands is somewhat surprising as no UPD peaks are seen in cyclovoltammograms obtained on the same systems studied by in situ STM (Fig. 2a–c). Typical Cu UPD peaks are observed on a bare electrode, but are suppressed on both thiol-modified electrodes. The exact reason for the formation of UPD islands is not clear, but the voltammograms clearly indicate that the islands are not formed by the deposition of Cu into thiol layer defects where the bare gold surface is exposed, acting as ultramicroelectrodes [26]. However, in the overpotential region, the voltammograms for the thiol-modified electrodes show that the bulk deposition is greatly inhibited by hexanethiol (Fig. 2b), and suppressed on octadecanethiol (Fig. 2c). In the former system, the deposition overpotential has been shifted cathodically by approximately 50 mV, and the small curvature after the deposition onset reveals that the reduction kinetics of Cu^{2+} have been substantially slowed. The voltammogram of Fig. 2c differs from previously published cyclovoltammograms of Cu deposition on octadecanethiol; those shown here are representative of defect-free layers where no macroscopic Cu deposits were observed. It should be mentioned that there is substantial variance of layer quality between samples.

Regarding Fig. 2b, the cathodic loop (larger cathodic current on the reverse scan and the subsequent crossing of the forward and reverse scans) is a signature of a nucleated deposition process, suggesting that Cu is being deposited on the hexanethiol layer, with charge transfer via electron tunneling across the organic layer to reduce the Cu^{2+} ions at the alkane/electrolyte interface [6,27]. This is consistent with UHV deposition studies where Cu was found to have a low penetration tendency on thiol monolayers [28]. With subsequent scanning (not shown), the cathodic current increases, indicative of incomplete stripping and the formation of new nucleation sites. Compared with the static deposition current estimated from surface coverage measurements calculated from Fig. 5 images (45 nA/cm^2), the dynamic deposition current density seen in the voltammogram of Fig. 2b at the same potential of −110 mV is greater. For octadecanethiol, the cyclovoltammogram in Fig. 2c shows no deposition characteristic. Evidently, a C_{18} layer is thick enough (25–30 Å [29]) to reduce the tunneling rate, hence, deposition rate, to an imperceptible level at the overpotentials covered within the scan range, provided it is defect-free. These data corroborate the above-mentioned observation of no Cu OPD under potentiostatic conditions on long chain ($n > 12$) alkanethiol layers.

On bare gold electrodes, overpotential (bulk) electrodeposition of Cu on Au(111) occurs by three-dimensional growth of islands on a UPD monolayer of Cu. The nucleation of 3D islands normally occurs at surface defects, such as step edges and kink sites at the gold surface. Self-assembled alkanethiol monolayers create a completely different growth scenario for Cu deposition on Au(111). Growth takes place exclusively on terraces, being nucleated at the UPD islands, a similar behaviour to that observed by Hölzle et al. [30] in the case of Cu deposition on Au(111) in the presence of thiourea.

Defect sites on the Au electrode are passivated by the alkanethiol. The 2D ramified morphology of the Cu deposition is evidence for the diffusion limited

[2] Based on a charge of 0.44 mC/cm^2 for a full 1×1 Cu monolayer on Au(111) [15].

aggregation of Cu adatoms once they are formed by Cu^{2+} ion reduction at the thiol–electrolyte interface. The growth, at least in the initial stages, occurs via a quasi two-dimensional mechanism. An important factor allowing this growth mechanism to be operative is certainly the slow growth kinetics on the alkanethiol modified electrodes. We attribute this to slow interfacial charge transfer, due to the addition electron tunneling barrier afforded by the alkanethiol layer, which also suggests that the Cu electrocrystallization occurs *on top* of the alkanethiol layer. The latter acts as a spacer layer through which electron tunneling must take place to pass charge across the interface with the electrolyte. If the electrodeposited Cu was in direct contact with the Au substrate, it would act simply as an extension of the electrode surface, causing surface roughening, thus enhancing the deposition rate over that on bare gold. This view is supported by the conclusions of a similar study [31]. A second important factor is the structural accommodation at the interface. A copper film growing pseudomorphically on the Au surface has a tensile strain of 13%. It might be possible that the "soft" thiol layer permits the copper to grow close to its natural lattice constant reducing Au–Cu misfit effects which would drive the system towards rough growth. We are currently preparing X-ray diffraction experiments to clarify this interesting point.

References

[1] G. Rosenfeld, N. Lipkin, W. Wulfhekel, J. Kliewer, K. Morgenstern, B. Poelsema, G. Comsa, Appl. Phys. A 61 (1995) 455.
[2] H. Röder, E. Hahn, H. Brune, J.P. Bucher, K. Kern, Nature 366 (1993) 141.
[3] M. Copel, M.C. Reuter, E. Kaxiras, R.M. Tromp, Phys. Rev. Lett. 63 (1989) 632.
[4] A.R. Despic, in: B.E. Conway, J.O'M. Bockris, E. Yeager, R.E. White (Eds.), Comprehensive Treatise of Electrochemistry, vol. 7, Plenum Press, New York, 1983, pp. 451–528.
[5] R.J. Nichols, W. Beckmann, H. Meyer, N. Batina, D.M. Kolb, J. Electroanal. Chem. 330 (1992) 381.
[6] H.O. Finklea, in: A.J. Bard and I. Rubenstein (Eds.), Electroanalytical Chemistry, vol. 19, Marcel Dekker, New York, 1996, pp. 109–335.
[7] O. Cavalleri, A. Hirstein, J.P. Bucher, K. Kern, Thin Solid Films 284/285 (1996) 392.
[8] S.E. Gilbert, O. Cavalleri, K. Kern, J. Phys. Chem. 100 (1996) 12123.
[9] K. Edinger, A. Golzhauser, K. Demota, C. Wöll, M. Grunze, Langmuir 9 (1993) 4.
[10] J.A.M. Sondag-Huethorst, C. Schönenberger, L.G.J. Fokkink, J. Phys. Chem. 98 (1994) 6826.
[11] J.P. Bucher, L. Santesson, K. Kern, Langmuir 10 (1994) 979.
[12] O. Cavalleri, A. Hirstein, K. Kern, Surf. Sci. Lett. 340 (1995) L960.
[13] G.E. Poirier, M.J. Tarlov, J. Phys. Chem. 99 (1995) 10966.
[14] O.M. Magnussen, J. Hotlos, R.J. Nichols, D.M. Kolb, R.J. Behm, Phys. Rev. Lett. 64 (1990) 2929.
[15] T. Hachiya, H. Honbo, K. Itaya, J. Electroanal. Chem. 327 (1991) 275.
[16] Z. Shi, J. Lipowsi, J. Electroanal. Chem. 365 (1994) 303.
[17] G.L. Borges, K.K. Kanazawa, J.G. Gordon, K. Ashley, J. Richer, J. Electroanal. Chem. 364 (1994) 281.
[18] L. Sun, R.M. Crooks, J. Electrochem. Soc. 138 (1991) L23.
[19] C.A. Widrig, C. Chung, M.D. Porter, J. Electrochem. Soc. 310 (1991) 335.
[20] J. Pan, N. Tao, S.M. Lindsay, Langmuir 9 (1993) 1557.
[21] N. Breuer, U. Stimming, R. Vogel, Electrochim. Acta 40 (1995) 1401.
[22] H. Brune, H. Röder, C. Boragno, K. Kern, Phys. Rev. Lett. 73 (1994) 1955.
[23] H. Brune, Ch. Romainczyk, H. Röder, K. Kern, Nature 369 (1994) 469.
[24] R. Hwang, J. Schröder, C. Günther, R.J. Behm, Phys. Rev. Lett. 67 (1991) 3279.
[25] J.A. Venables, G.D.T. Spiller, M. Hanbücken, Rep. Prog. Phys. 47 (1984) 399.
[26] O. Chailapakul, R.M. Crooks, Langmuir 9 (1993) 884.
[27] J. Lipkowski, in: B.E. Conway, J.O'M. Bockris, R.E. White (Eds.), Modern Aspects of Electrochemistry, vol. 23, Plenum Press, New York, 1992, pp. 1–90.
[28] D.R. Jung, A.W. Czanderna, Crit. Rev. Solid State Mater. Sci. 19 (1994) 1.
[29] M.D. Porter, T.B. Bright, D.L. Allara, C.E.D. Chidsey, J. Am. Chem. Soc. 109 (1987) 3359.
[30] M.H. Hölzle, C.W. Apsel, T. Will, D.M. Kolb, J. Electrochem. Soc. 142 (1995) 3741.
[31] J.A.M. Sondag-Huethorst, L.G.J. Fokkink, Langmuir 11 (1995) 4823.